3.4. Measurement of polymer degradation by CL, TGA, DSC, Py-GCMS and SPME-GCMS

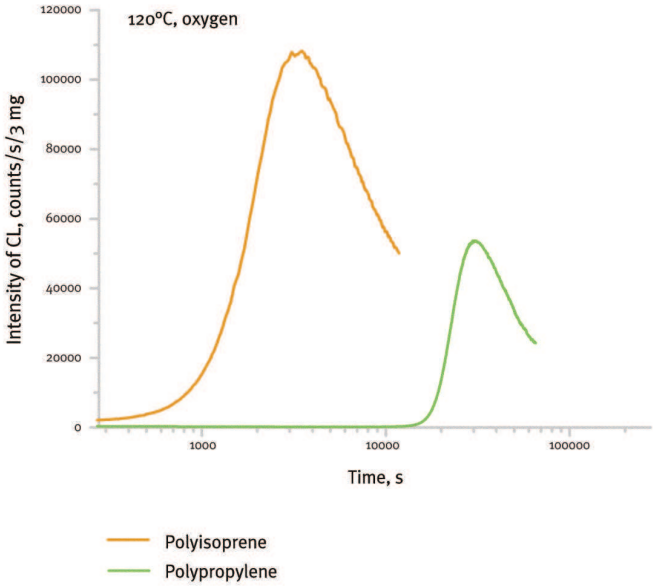

Figure 8. Comparison of chemiluminescence runs from saturated and unsaturated pure hydrocarbon polymers having tertiary carbons (polypropylene, polyisoprene) in the main chain

The plastics used for the degradation studies were either pure polymers used either as films or powders. As a representative set of plastics in the study, commercially available the so-called ResinKit™ published and distributed by the ResinKit™ company (Woonsocket, RI, USA). It includes 50 of the most frequent polymers containing different additives. Some plastics from this set became the items in the SamCo collection described in the Chapter 1.

Figure 8 shows how the elementary structure of the polymer affects the observed patterns of chemiluminescence response in oxygen at 120°C. As expected, the degradability decreases in the order polyisoprene < polypropylene in correspondance with the amount of C=C and tertiary carbon atoms in the polymer structure.

The intensity of chemiluminescence signal from a heated polymer and the kinetics of its change with time or temperature is determined by:

- the quality of the polymer, its photo-oxidation and thermo-oxidation history expressed in concentration of hydroperoxides, carbonyl groups or of other oxidized structures and terminal groups. The rate of an oxidative attack may then be related to the average molar mass and to its distribution, and to the ratio of amorphous/crystalline structures. Polymers cannot be simply ordered according to the intensity of light emission at a given temperature. The chemiluminescence-time patterns are related with the rate of sample oxidation, but they may differ from one to the next polymer.
- the quality of the polymer surface; for example, for a particular polymer the intensity of the signal will be different for film and for powder.

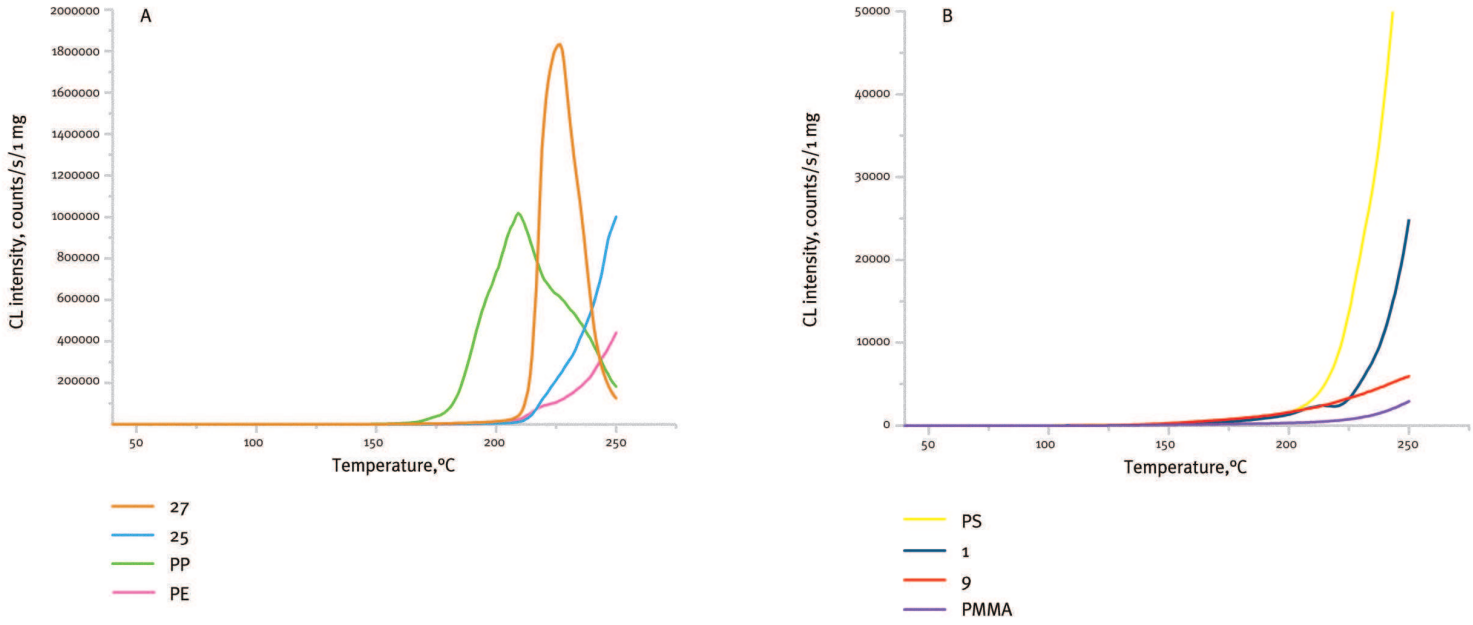

Figure 9. Non-isothermal chemiluminescence runs for polypropylene (PP), polyethylene (PE) (part A of the graph), polystyrene (PS) and poly(methyl methacrylate) (PMMA) (part B of the graph). Numbers 27, 25, 1 and 9 denote the sample of the same polymers from the ResinKit™. The rate of heating 5°C.min^{-1}, oxygen

- the temperature and concentration of oxygen in the atmosphere surrounding the oxidised sample.
- the extent and quality of polymer stabilisation.
- a direct oxidation of polymer additive, which may occassionaly give a much stronger signal than the oxidation of polymer itself. This is vey important as it may lead to an erroneous relation between the rate of polymer oxidation and chemiluminescence intensity.

An oxidation test involving temperature ramp experiments in oxygen over a temperature range 40–220°C enables one to compare the degradability of different materials over a large temperature interval from the viewpoint of their chemiluminescence intensity.

In the Figure 9 we may see the comparison of the chemiluminescence runs for pure polypropylene, polyethylene, polystyrene and poly(methyl methacrylate) and corresponding polymers from the ResinKit™ (27, 25, 1 and 9). The information that may be obtained from this comparison is as follows: as the line 27 is shifted to significantly higher temperatures, PP 27 from the resin kit is heavily stabilised. At the same time polymer fragments which are formed in degradation in oxygen have substantially lower molar mass. PE 25 is stabilised only slightly but the degradation products have again lower molar mass than it is in the case of pure polyethylene. The shift to higher temperatures and some extent of polymer stabilisation may be observed also in the case of PS 1 but the products of degradation have higher molar mass than

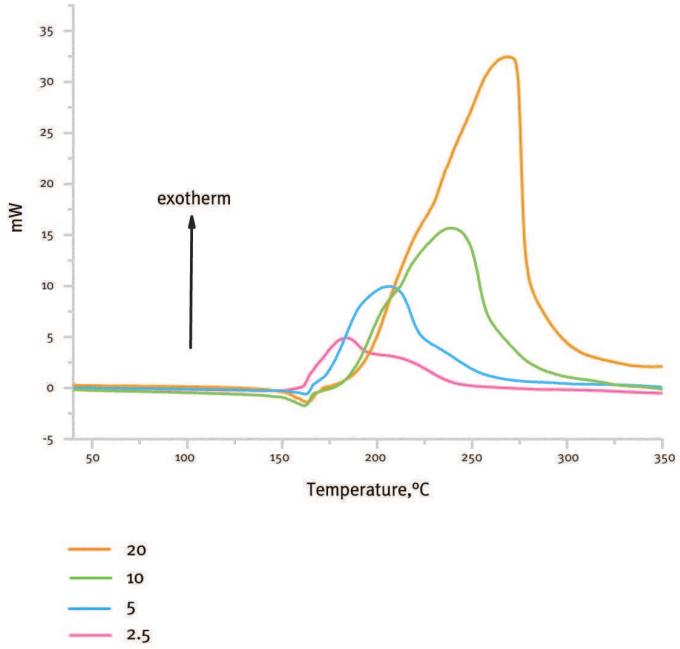

Figure 10. DSC course of oxidation of polypropylene powder, oxygen. Numbers denote the rate of heating in °C.min^{-1}

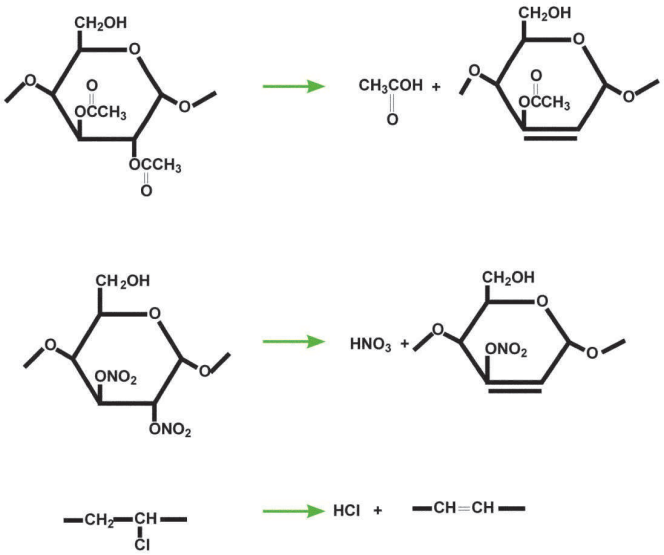

Figure 11. Primary step of formation of acids from elementary units of cellulose acetate, cellulose nitrate and poly(vinyl chloride)

the reference sample while PMMA 9 from the resin kit denoted as acrylics degrades even faster than the reference sample.

The important parameter which affects the position and shape of the corresponding non-isothermal records of degradation of polymers is the rate of sample heating (Rychlý 2011, b). As it may be seen in the Figure 10 the DSC exotherms of polypropylene in oxygen are shifted to higher temperatures and become more distinct due to the increasing rate of heating. However, this is valid for case of non-isothermal thermogravimetry in nitrogen and DSC and chemiluminescence from polyolefins in oxygen. In the former case it is even used for calculation of activation energy of polymer degradation. There are polymers such as poly(methyl methacrylate), polystyrene and others for which this shift is insignificant and/or cannot be observed at all.

3.4.1. Polymers that can damage other objects ("malignant" polymers)

3.4.1.1. Cellulose derivatives and poly(vinyl chloride) (PVC)

The first step of the unzipping process leading to the formation of ethanoic acid, nitric acid and hydrogen chloride from such kind of polymers is seen on the Figure 11.

Nitric acid is a strong oxidising acid which causes tendering and decomposition of cellulose and proteins, and corrosion of metals. Cellulose acetate produces ethanoic acid (vinegar odor, hence the term "vinegar syndrome" to describe cellulose acetate degradation) and cellulose butyrate and cellulose acetate butyrate produce butyric acid which has a distinctive and characteristic vomit odour. These organic gases are not as harmful as nitric acid, but they also cause tendering, decomposition, and corrosion. Particularly corrosive effects are performed by hydrogen chloride.

Cellulose nitrate (nitrocellulose, flash paper) is a highly flammable compound formed by nitrating cellulose through exposure to nitric acid or another powerful nitrating agent. When used as a propellant or low order explosive, it is also known as guncotton. Nitrocellulose plasticised by camphor was used by Kodak, and other suppliers, from the late 1880's as a film base in photographs, X-ray films and motion picture films; it was known as "Nitrate film". After numerous fires caused by unstable nitrate films, safety film started

to be used from the 1930's in the case of X-ray stock and from 1948 for motion picture film, as well.

Cellulose nitrate is found in many older artefacts, including sheets or films (e.g., photographic film base), varnishes and lacquers, and solid objects, especially those which imitate natural materials like ivory (often called "French ivory"), tortoiseshell, and horn. Cellulose nitrate degrades to produce acidic and nitrogen oxide gases which can seriously damage objects that are nearby or in contact. This deterioration is accelerated by increased temperatures, by elevated relative humidity, and by acidic conditions. It may be even said that it is a merit of cellulose nitrate artefacts in museums which brought about an increased attention to museum's objects from plastics as such.

Cellulose acetate is commonly encountered in two grades characterised by different degrees of substitution, namely, cellulose triacetate most commonly found in sheets like photographic film base and fibers, and cellulose diacetate in thicker sheets and three dimensional shapes and objects often simulating tortoiseshell, ivory, wood, and mother-of-pearl. The cellulose triacetate and diacetates are easily confused with cellulose nitrate when compared by visual appearance alone. Cellulose acetate objects usually contain plasticisers. Cellulose acetate degrades primarily by acid hydrolysis, which causes deacetylation (Figure 11). Deacetylation cleaves pendant acetate groups from the cellulose polymer backbone and depolymerises the backbone. Formation of ethanoic acid from the plastic creates the acidic surfaces on the plastic and acidic atmospheres in enclosures. This process is analogous to that which happens with cellulose nitrate. Depolymerisation leads to decrease in mechanical strength and fracture plus deformations and warpage. Ethanoic acid diffuses through the display or storage space, and can cause corrosion of metals, or acidic catalysed degradation of other paper and textiles. Additives, especially plasticisers, migrate and may be lost, or are hydrolysed or oxidised to acidic compounds. This leads to warpage, embrittlement, and fracture, and to the development of acidic and sticky surfaces, sometimes with surface deposits of plasticiser or acidic degradation products.

Pure poly(vinyl chloride) (PVC) degrades to produce hydrogen chloride at temperatures needed to form it into usable products by molding or extrusion. As a consequence, heat stabilisers are always added to overcome this problem. As pure poly(vinyl chloride) is a rigid plastic compounds called plasticisers are added to convert it into flexible plastic. Plasticisers are typically oily polar organic liquids, which are very good solvents for many materials.

Polymer	α_1, predominating fraction of volatiles	k_{av}, 40°C, s^{-1}	k_1, 40°C, s^{-1}	k_{av}, 100°C, s^{-1}	k_1, 100°C, s^{-1}
Nitrate of cellulose	0.53	1.3e-5	6.6e-21	2.6e-5	6.4e-12
Polyvinyl chloride	0.54	2.8e-7	7.5e-12	2.0e-6	1.7e-8
Polyurethane, ester	0.64	3.7e-11	2.2e-14	3.0e-8	8.0e-11
Acetate of cellulose	0.81	3.8e-8	1.9e-23	2.3e-7	7.9e-17

Figure 12. Rate constants of decomposition of some malignant polymers into volatiles as determined by nonisothermal thermogravimetry in nitrogen (k_1) and by chemiluminescence in oxygen (k_{av})for 40 and 100°C

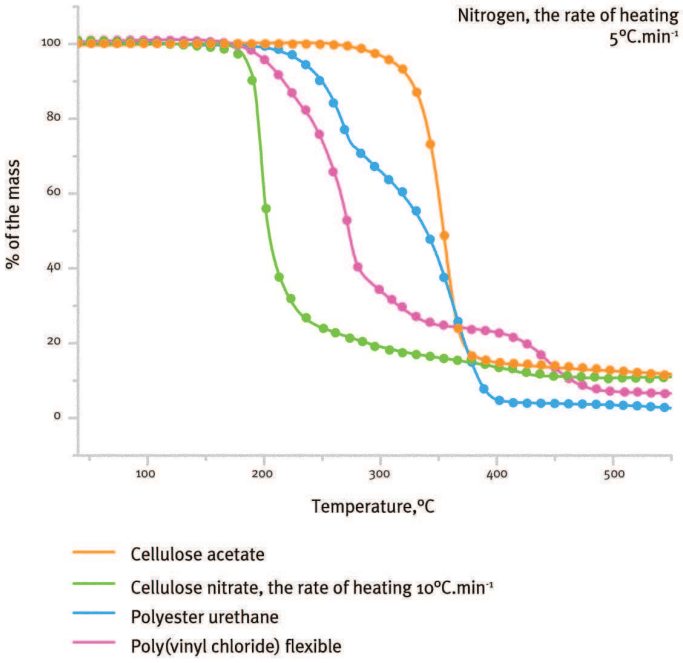

Figure 13. Nonisothermal thermogravimetry runs in nitrogen of malignant polymers. Points denote the theoretical fit according to the Eq. 14. Cellulose acetate was powdered sample, polyester urethane and cellulose nitrate are referred to below and poly(vinyl chloride) is SamCo 37 sample

The release of volatiles from the above polymers is seen in the Figure 13. Nitrate of cellulose is the least stable, then it is followed by poly(vinyl chloride), polyester urethane and acetate of cellulose. The rate constants k_1 determined from the theoretical fits by eq. 14 for j=3 and 40 and 100°C are in Figure 12 while activation energies for the release of predominating fraction of volatiles are 337, 126, 133 and 248 $kJ.mol^{-1}$ for nitrate of cellulose, poly(vinyl chloride), polyester urethane and acetate of cellulose, respectively. It may be of interest that in the sequence of stability at low temperatures according to the rate constants polyester urethane is more stable than acetate of cellulose. However, this is not the case when we consider the stability at the higher temperature region involving the fraction of the polymer which yields the prevailing amount of volatiles. High activation energies of the volatile release indicates the run typical for the explosion like course of cellulose nitrate degradation.

The non-isothermal chemiluminescence curves in oxygen for the same polymers are seen in the Figure 14. The sequence of stability is: cellulose nitrate < poly(vinyl chloride) < polyester urethane < acetate of cellulose and corresponds to that in the nitrogen atmosphere from thermogravimetry experiments regardless of the fact that the average rates constants determined by means of eq. 11 and 12 are higher because of the oxygen.The chemiluminescence runs of degradation of nitrocellulose involve typically the decomposition peak A of the cellulose nitrate itself which is followed by the peak B monitoring the oxidation of the char residue being formed from original cellulose nitrate.

In the Figure 15 we see the comparison of stabilities of different acetates of cellulose from the ResinKit™ collection as determined by chemiluminescence and thermogravimetry under non-isothermal conditions; the sequence is in both kinds of experiments the same and corresponds to the order:

cellulose acetate propionate < cellulose acetate butyrate < cellulose acetate

Cellulose nitrate examined in the next experiments was a white membrane used in biology; it is produced by GE Healthcare (US).

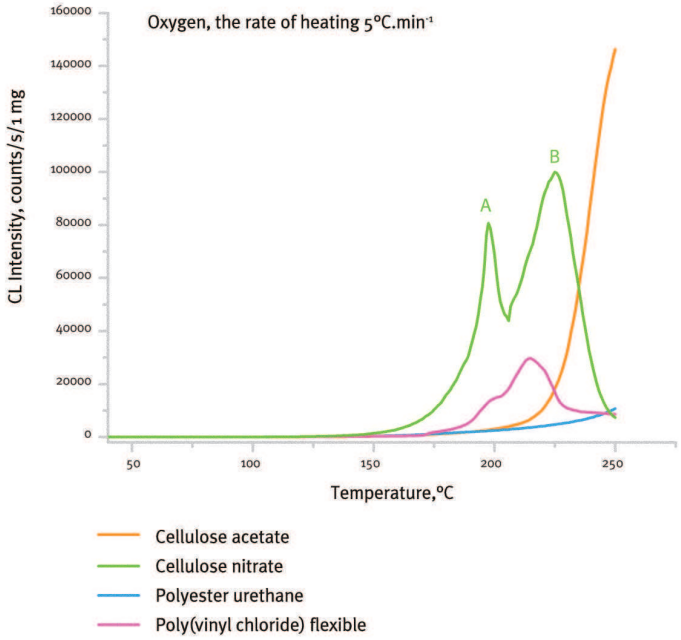

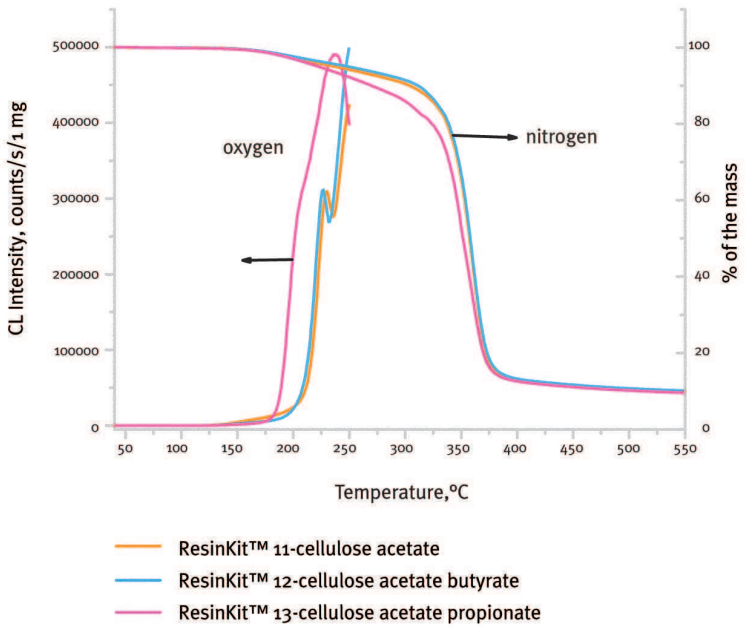

Figure 14 (left). Nonisothermal chemiluminescence runs of polymers in oxygen from the Figure 13

Figure 15 (right). Nonisothermal chemiluminescence in oxygen and thermogravimetry in nitrogen for different acetates of cellulose

The quantitative elemental analysis indicated a weight percent of carbon, hydrogen and nitrogen 27.20, 2.93 and 11.76%, respectively. Cellulose nitrate contained two nitro groups per one glucopyranosyl unit of the cellulose. The samples were aged for periods varying from 6 hours until 16 days at 130°C in open conditions of ambient air and uncontrolled relative humidity. The aged samples were collected at intervals 6 hours, 1 day, 2 days, 4 days, 8 days and 16 days, respectively. Visual observation confirmed the increase of the yellowing with time of ageing already after 2 days of ageing. The samples became slightly brown after 4 days of ageing and dark brown when aged longer. Due to ageing nitrocellulose becomes brittle. The formation of acid volatiles was evaluated by pH measurements of aqueous extract (1.5 mg of sample was immersed in 150 µl of pure water with a stirring bar, during 3 hours). This extract became significantly acidic with the duration of ageing. The pH changed from 6.5 (for the reference sample) to 2.5 (for 16 days-aged sample). The pH values obtained after 1 day, 2 days, 4 days and 8 days were 4.8, 4.7, 3.5 and 3.0, respectively.

From the Figure 16 it may be seen how nitration destabilises the original cellulose. The effect of oxygen on the degradation of nitrocellulose is not almost visible on thermogravimetry experimental runs while that for pure cellulose it is significant. This may be explained by the intervention of oxygen into the initiation reaction of oxidation via the carbon atom 6 of glucopyranosyl unit of the cellulose while in the case of nitrocellulose the initiation occurs

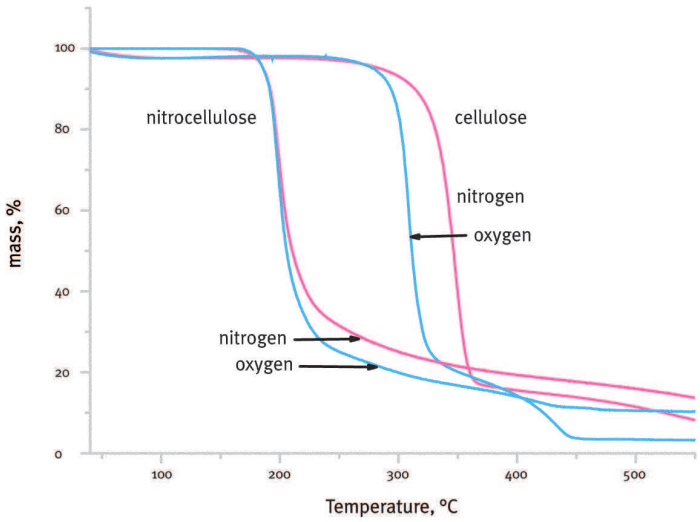

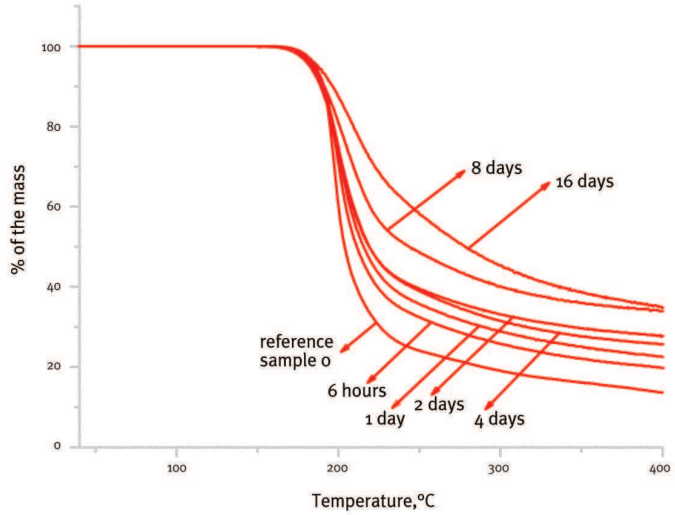

Figure 16 (left). Comparison of nonisothermal thermogravimetry runs of cellulose and nitrocellulose in nitrogen and oxygen. The rate of heating 10°C.min^{-1}

Figure 17 (right). Comparison of non-isothermal thermogravimetry runs of aged nitrocellulose samples, nitrogen, the rate of heating 10°C.min^{-1}

independently via the scission of bonds –O-NO_2. Oxygen affects the oxidation in the subsequent stages of the reaction. The loss of volatiles is also much sharper for nitrocellulose than for cellulose. At high temperatures there remains a certain amount of char residue which under nitrogen looses the weight slowly. In oxygen an acceleration of the char residue oxidation may be observed above 420°C.

Non-isothermal thermogravimetry runs of the set of cellulose nitrate in nitrogen at the rate of heating 10°C.min^{-1} are seen in the Figure 17. It is worth of noticing that with the progress of the sample ageing at 130° C in air the temperature of the inflexion point shifts to higher values being 197.7°C for reference sample and 207.7°C for the most aged sample. This corresponds with the gradual loss of nitro groups from cellulose nitrate due to ageing. At the same time the percentage of the char residue which remains after thermogravimetry experiment at 550° C slowly increases.

The set of parameters obtained from non-isothermal thermogravimetry experiments (eq. 14) such as the activation energy and fractional values α of respective components released as volatiles or remaining as a char residue is given in the Figure 18. Activation energy estimated according to eq.14 for release of volatiles decreases with the progress of nitrocellulose ageing being 260 kJ.mol^{-1} for the reference and 130 kJ.mol^{-1} for the sample aged 16 days in air at 130°C. At the same time, the rate constants k_2 calculated from Arrhenius parameters for 130°C increase with the extent of nitrocellulose ageing.

The Figure 19 brings an overview of the rate constants of nitrocellulose decomposition determined from TG, DSC and

Aged at 130°C, days	α_2	E_2 kJ.mol^{-1}	τ_2, at 130°C, days
0	0.713	201.1	7.6
0.25	0.645	160.5	2.1
1	0.618	142.1	1.2
2	0.589	137.0	0.84
4	0.596	124.6	0.62
8	0.520	102.7	0.35
16	0.489	66.1	0.14

Figure 18. Parameters of degradation of aged nitrocellulose from non-isothermal thermogravimetry (eq. 14) – α_2 is the predominating fraction of volatiles formed, τ_2 is the corresponding half-life (τ_2=0.693/k_2), k_2 and E_2 are corresponding rate constants and the activation energy, respectively

k, s^{-1} 50°C	k, s^{-1} 130°C	k, s^{-1} 200°C	Note
1.3e-15	2.6e-7	0.0229	reference sample 0, TG in nitrogen
-	5.0e-9	0.0095	reference sample 0, DSC in nitrogen
2.0e-9	4.5e-6	0.0032	reference sample 0, CL in nitrogen
4.2e-8	3.1e-6	-	sample aged 6 hours in air, CL in oxygen
-	1.2 e-6	-	Surface below DSC curves of aged samples, air
1.3e-8	3.8e-5	0.0044	sample 16 days aged in air, oxygen, faster reaction
5.0e-9	1.4e-5	0.0015	sample 16 days aged in air, oxygen, slower reaction
1.6e-11	6.0e-6	0.0083	(Binke *et al.* 1999)
1.2e-10 (below 80°C)	2.9e-6 (above 100°C)	7.8e-3	(Volltrauer and Fontijn 1981)
5.0e-9	5.1e-4	0.493	ASTM method (Pourmortazavi *et al.* 2009)
7.0e-9	5.7e-4	0.489	Method by Ozawa (Rong *et al.* 1999)

Figure 19. Rate constants of the first order of the nitrocellulose degradation exposed to ageing obtained by the different approach

chemiluminescence runs for 50, 130 and 200°C, respectively. While relatively good agreement may be seen for 200°C with the exception of data from the papers (Pourmortazavi 2009; Rong 1999) which provide much higher values, the temperature close to ambient (50°C) gives the span over several orders of magnitude which are typical particularly for non-isothermal TG and DSC measurements. Even data corresponding to temperature 130°C (the temperature of ageing) are not very far each from the other. It may be of interest that the rate constants from thermogravimetry increase with the extent of sample ageing. This fact should be considered when treating different cellulose nitrate samples of the different storage history.

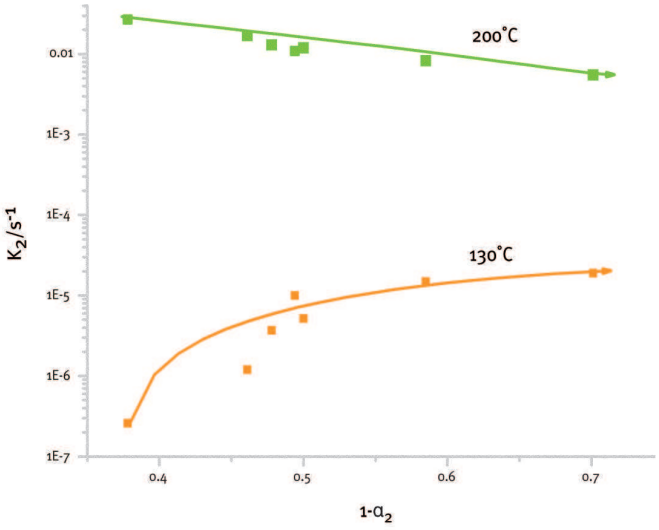

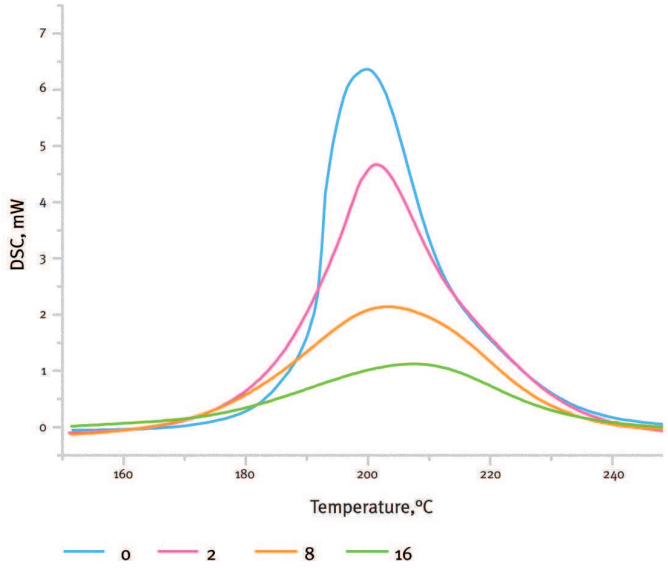

Figure 20 (left). The correlation of the rate constants approximated from the set of experiments (Figure 17 and Figure 18) with a char residue $1-\alpha_2$

Figure 21 (right). Example of non-isothermal DSC runs in nitrogen of aged samples of cellulose nitrate, the rate of heating 5°C.min^{-1}. The numbers denote the days of sample ageing at 130°C

The rate constants of the first order determined from the parameters of the fit using eq. 14 for 130 and 200°C correlate with the percentage of the char residue determined from non-isothermal TG runs; those at 130°C with an increasing percentage of the char residue increase (Figure 20). Although the extrapolation of rate constant to 130°C from non-isothermal TG is affected by the faster auto accelerating decomposition process occurring above 190°C, the increasing tendency of the rate constants indicate that there may occur the effect of the forming char on the autocatalysis of decomposition of nitrocellulose. Until now the autocatalysis in decomposition of cellulose nitrate was ascribed to the effect of nitric acid. From the flammability experiments on some energetic materials we know that the glowing char may act as a spark of the ignition of the explosive course.

With the extent of nitrocellulose ageing there also occurs a shift of the maximum of DSC exotherm to higher temperatures while the peak height is reduced (Figure 21). The essential data from DSC measurements in nitrogen for the rates of heating 5 and 10°C.min^{-1} are summarized in the Figure 22 indicating quite a good repeatability of respective experiments. As expected, the maximum of the exotherm is shifted to higher temperatures for the higher rate of heating.

Provided that the surface below DSC exotherm is proportional to the concentration of unreacted nitro groups and the kinetics of nitrocellulose decay in membrane during its ageing at 130°C is approximated by the first order scheme (Figure 23) we see that the rate constant of nitrocellulose degradation is somewhat lower than

Days of sample ageing at 130°C	Surface below the exotherm/ Jg^{-1}		Peak height/ Wg^{-1}		Temperature of the peak/ °C	
	$5°C.min^{-1}$	$10°C.min^{-1}$	$5°C.min^{-1}$	$10°C.min^{-1}$	$5°C.min^{-1}$	$10°C.min^{-1}$
0	1870	1723	6.65	11.35	200.07	207.8
	1718	1969	6.17	12.05	199.96	208.8
0.25	2029	1858	6.82	12.24	199.93	207.45
	1964	1811	6.55	11.54	199.46	207.10
1	1719	1845	5.62	10.9	200.57	206.5
2	1746	1895	5.02	9.26	201.03	207.5
	1696	-	4.70	-	201.95	-
4	1319	1673	3.13	8.00	201.22	207.6
	1274	1489	3.30	7.51	201.18	207.7
8	1144	1292	2.39	4.41	203.2	210.8
	972	1401	2.13	4.61	202.52	210.8
16	521.90	779	1.08	2.2	207.84	218.9
	759.40	653	1.32	2.2	206.82	215.5

Figure 22. DSC parameters for the aged nitrocellulose – comparison of parallel experiments in nitrogen at the rate of heating 5 and $10°C.min^{-1}$

that found by extrapolation from chemiluminescence measurement. However, the difference is not as large (Figure 19).

Regardless of the observations provided by thermogravimetry namely that the effect of oxygen on nitrocellulose degradation is not as distinct as it is in the case of cellulose it still exists. In Figure 24 we may see the comparison of DSC exotherms for the rate of heating $5°C.min^{-1}$; the surface below DSC exotherm in nitrogen is 66% of that for oxygen.

When comparing DSC and chemiluminescence runs in oxygen we see another peak (See also peak B in the Figure 14) appearing in the latter case (Figure 25) which is likely to correspond with the oxidation of char residue. In nitrogen experiments this peak was not observed. We may also see that in the presence of nitrogen the chemiluminescence signal, that is lower than in oxygen, is also important.

Figure 26 shows how chemiluminescence intensity changes with the stepwise increase of temperature. The experiment was performed so that temperature was kept constant for a certain time

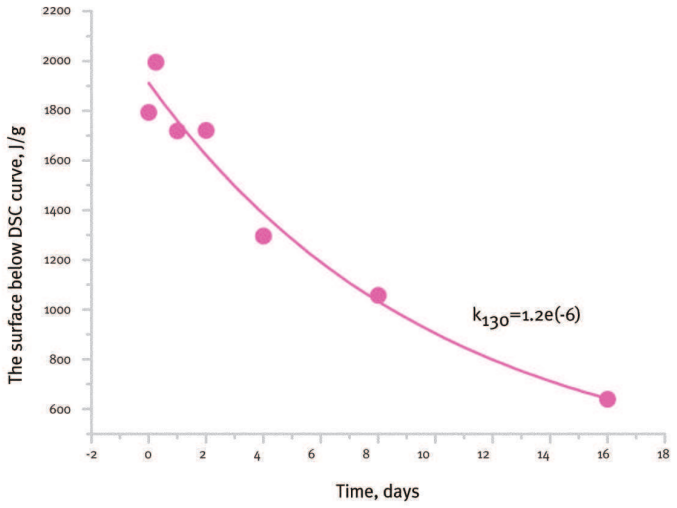

Figure 23. The decay of the surface below DSC exotherms of the cellulose nitrate aged in air at 130°C

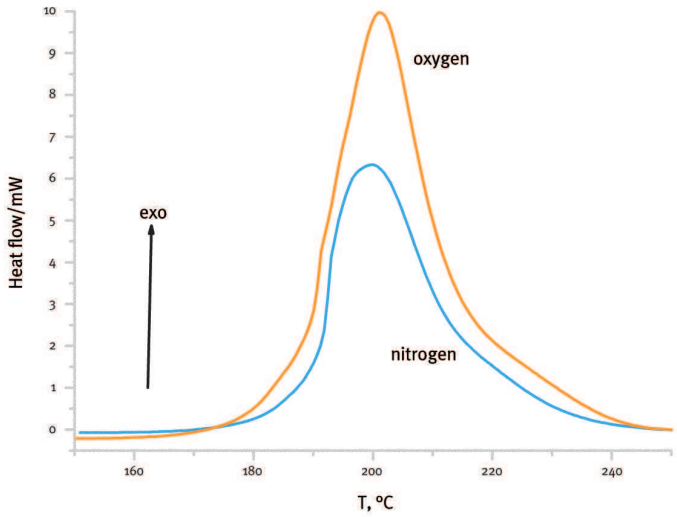

Figure 24. Comparison of DSC runs for nitrocellulose (reference sample o) in oxygen and in nitrogen. The rate of heating 5°C.min^{-1}

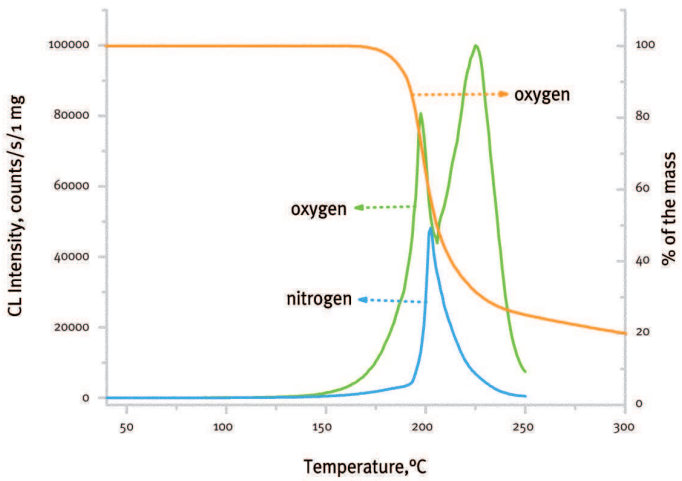

Figure 25. Non-isothermal chemiluminescence runs in oxygen and nitrogen (the rate of heating 5°C.min^{-1}) and thermogravimetry run in oxygen (the rate of heating 10 °C.min^{-1}) for reference sample (sample o) of nitrocellulose

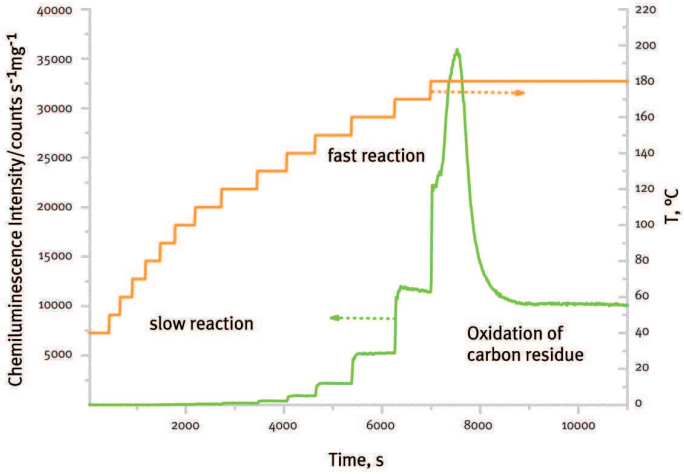

Figure 26. Chemiluminescence–stepwise increase of temperature for nitrocellulose sample

and the chemiluminescence run in oxygen occurred isothermally. The fast increase of chemiluminescence intensity took place already at 180°C. At lower temperatures the isothermal parts of the decomposition curve gave the stationary levels of the intensity of light emission eventually being accompanied by the slow decay. This experiment also serves as an elegant combination of isothermal and non-isothermal experiments for a fast assessment of plastic stability.

The temperature interval well below 190°C which corresponds to the activation energy 89 kJ.mol^{-1} gives evidently good rate constants

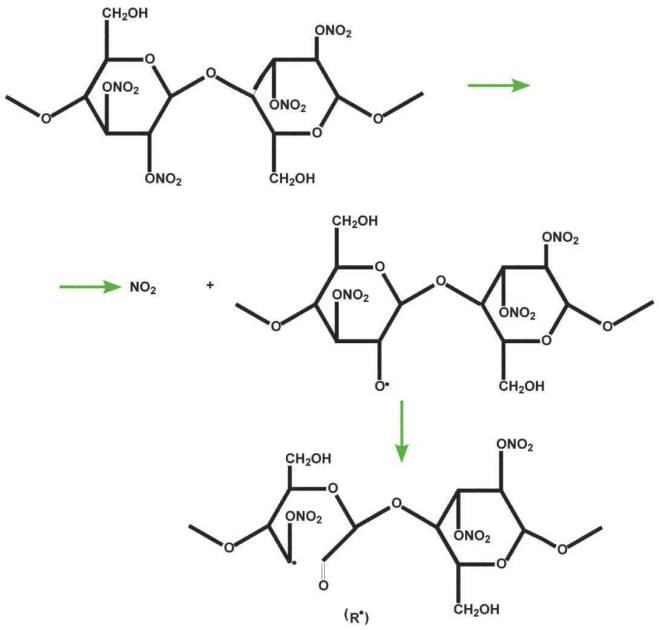

Figure 27. Initial stages of the decomposition of cellulose nitrate

when extrapolating to lower temperatures (Figure 19). This allows to predict the remaining service life of the cellulose nitrate more reliably.

There are no doubts that the initial step in degradation of nitrocellulose is the splitting of –O-NO_2 bonds of the secondary nitrate group joined to carbon atoms 2 or 3 of the glucopyranosyl ring (Figure 27). These bonds have the dissociation energy 167 kJ.mol^{-1} while those at the primary position of carbon atom 6 have dissociation energy about 330 kJ.mole^{-1} (Shashoua 2008). The subsequent steps are more the matter of speculation, especially those leading ultimately to a char. One possibility is that in the sequence of β-scissions glucopyranosyl ring may open, the free radicals R$^{\cdot}$ split out another molecule of NO_2 and finally there appear aldehydes, which are prone to oxidation due to direct reaction with oxygen or in its absence with NO_2. The transfer reaction to CH_2 bonds on carbon atoms 6 may induce the splitting off the formaldehyde (Figure 27). Nitric acid which is formed from NO_2 due to the presence of air humidity will contribute to the cation induced cleavage of glycosidic bonds C-O-C linking glucopyranosyl units and the molar mass of nitrocellulose is reduced. At the same time, after decarbonylation of aldehydic groups the following sequential moieties in the nitrocellulose macromolecules may be formed which form the possible skeleton of the char formed.

3.4.1.2. Polyurethanes (PUR)

Polyurethane foams are widely present in museum collections either as a constituent of the museum artefacts or as a material for their conservation (stuffing, protection, packing and storage) (Waentig 2008, 301; Quye and Williamson 1999). Among museum collections they feature predominantly as sculptures, design objects, cushioning materials, textiles, and toys. Today many of polyurethane foam artefacts are in poor condition and often exhibit specific conservation issues. Instability of polyurethane foams has been recognized although it mainly depends on the raw materials used during manufacturing. There are two types of polyurethane foams: one based on polyether polyols and the other based on polyester polyols. The polyether polyurethanes are particularly susceptible to oxidation. Oxidation is initiated and accelerated by exposure to light, especially UV radiation (Szycher 1999). Foam degradation is particularly devastating usually leading to complete crumbling of the foam object starting at its surface. Polyester urethanes are much less susceptible to oxidative degradation, but are subject to hydrolytic degradation at high relative humidity. Coated and painted foams

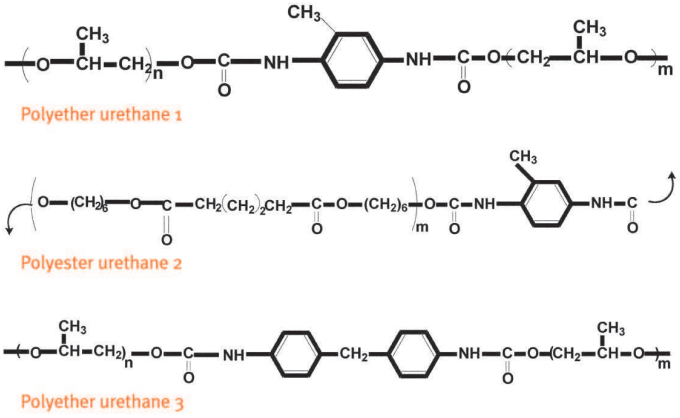

Figure 28.The predominant structures in polyurethanes examined

were found to be more resilient because they have a protective barrier against oxygen.

Three structures of polyurethanes were examined as seen below (Figure 28), namely polyether urethane having toluene (TDI) and diphenyl methane diisocyanate (MDI) moieties (Sample 1 and 3) and polyester urethane (Sample 2) with toluene diisocyanate (TDI) units (Rychlý 2011a).

These polyurethanes foams were supplied by RAJA Company, France. The foams were subjected to light ageing under daylight 1000 Wm^{-2}, 25°C/50% relative humidity or thermal ageing under dry (90°C, <10% RH) or humid (90°C, 50% RH) conditions.

Thermal oxidation of polyester based polyurethanes starts in polyisocyanate segments, probably on methylene units adjacent to NH groups. This was confirmed by experiments of chemiluminescence in oxygen of either polyisocyanate or polyol in comparison to polyurethane prepared from the two components. The light emission uptake from polyisocyanate precedes that from polyester polyol. A similar pattern, however, shifted to higher temperatures, was revealed by nonisothermal thermogravimetry in nitrogen (Ravey 1997).

Polyester urethane storage during 18 months leads to a considerable change of the chemiluminescence versus temperature pattern. The sample became less thermally stable in oxygen and the intensity of the light emission was also lower. At the same time, the molar mass distribution of the polyol did not change.

The contact with tap water of a polyurethane film cast on glass caused a reduction of the themooxidative stability of polyurethane. This was attributed to the combined effect of hydrolysis and ions present in the water (Gajewski 1990).

The simple and fast differentiation between polyether and polyester urethanes realized through the thermooxidation experiment performed on chemiluminescence device may be seen in the Figure 29. Polyether urethanes due to the ether structures $–CH_2$-O- and much easier oxidation perform considerably higher light intensity at final stages than polyesther urethane. However, the degradation of the latter starts earlier. In one of our papers (Malíková 2010) we have shown that the development of the chemiluminescence follows after the release of the nitrogen containing moieties and is linked with the oxidation of the crosslinked structures in the polymer.

Differentiation of degradation pattern of polyether and polyester urethanes as seen by thermogravimetry in oxygen and nitrogen is shown in the Figure 30. Polyester urethane in oxygen undergoes the extensive crosslinking which is accompanied by carbonisation

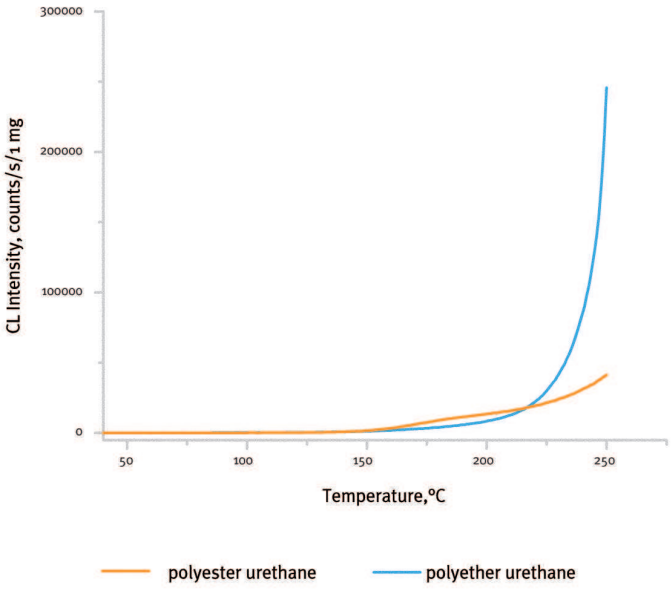

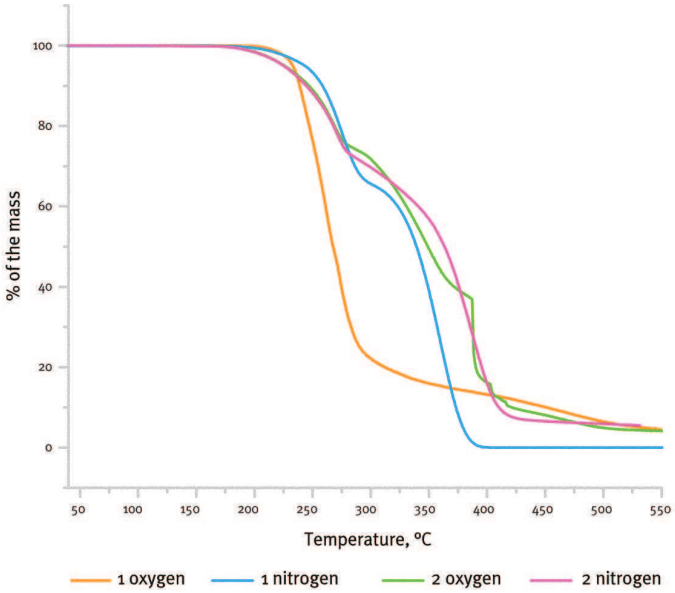

Figure 29. Chemiluminescence from polyurethanes, non-aged samples of polyether urethane and polyester urethane, oxygen, the rate of heating 5°C.min^{-1}

Figure 30. The comparison of nonisothermal thermogravimetry for polyether urethane (line 1) and polyester urethane (line 2) in nitrogen and oxygen, the rate of heating 5°C.min^{-1}

of the superficial layers and sudden release of volatiles at elevated temperature.

The mutual links of the outputs of respective methods (thermogravimetry, DSC, chemiluminescence) are seen in Figures 31 and 32. DSC endotherms in nitrogen (Figure 33) represent the records of the active decomposition of both polyurethanes into volatiles and again confirm the essential differences in polyether and polyester urethanes degradation.

Figure 34 shows non-isothermal thermogravimetry records of original polyurethane samples 1 and 2 and those aged by light. The differences are significant, indeed. While original polyurethane foams give in nitrogen two waves of the formation of volatiles which were ascribed to the decomposition of polyisocyanate (the first) and polyol or/polyester (the second) moieties, aged polyether samples give only one wave of the decay of the mass (1a). The aged polyether samples (1a) are already disintegrated. Polyester urethanes (2) start to loose volatiles from polyisocyanate moieties at lower temperatures but the mass loss from polyester part is shifted to higher temperature when compared with polyether urethanes 1. Typically much more carbon residue remains on the pan for aged samples (Figure 35) which indicate the additional crosslinking in polyol or polyester part of polyurethane provoked by ageing.

Also chemiluminescence – temperature records in oxygen are significantly changed by polyurethane ageing (Figure 36). While sample 1a shows a maximum, the samples 2a and 3a give an increased light intensity at lower temperatures when compared

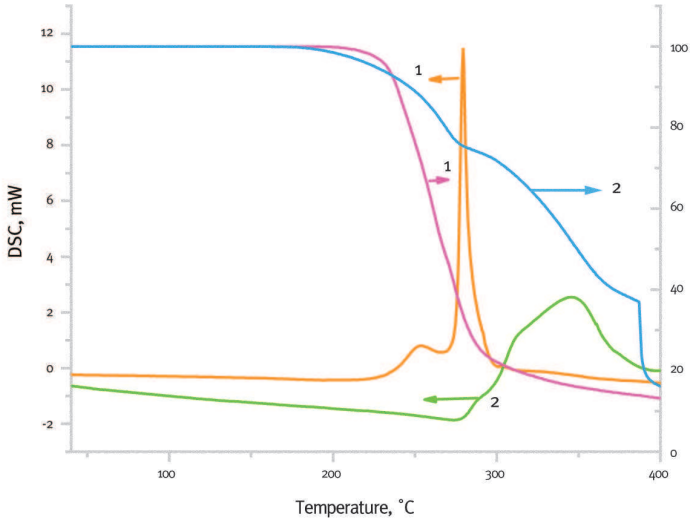

Figure 31. Comparison of nonisothermal thermogravimetry and DSC records for polyether (the lines 1) and polyester (the lines 2) urethane foams, oxygen, the rate of heating 5°C.min^{-1}

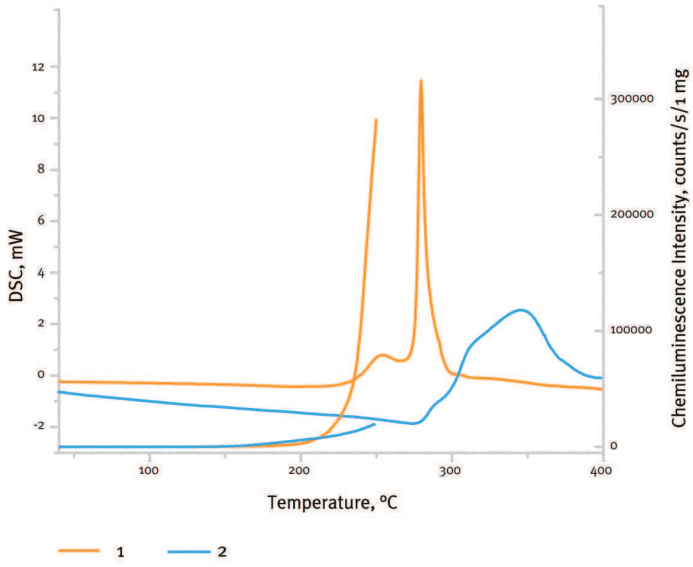

Figure 32. Chemiluminescence and DSC measurements in oxygen for non-aged polyether urethane (1) and polyester urethane (2). The rate of heating 5°C.min^{-1}

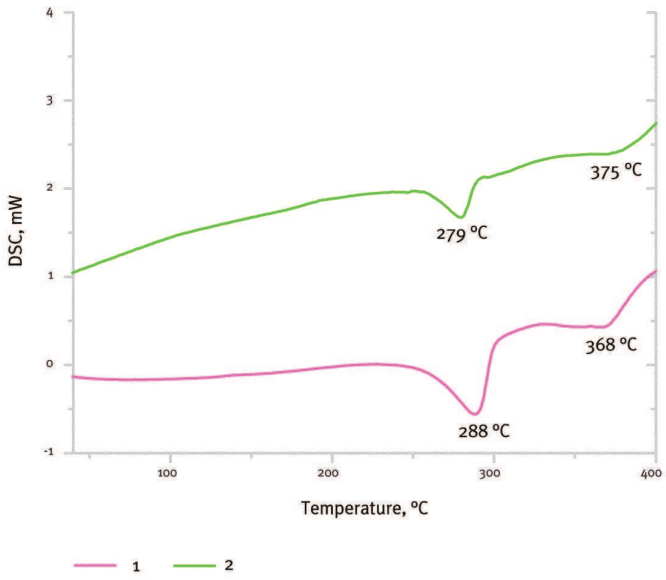

Figure 33. Comparison of non-isothermal DSC records of polyether urethane (1) and polyester urethane in nitrogen. The rate of heating 5°C.min^{-1}

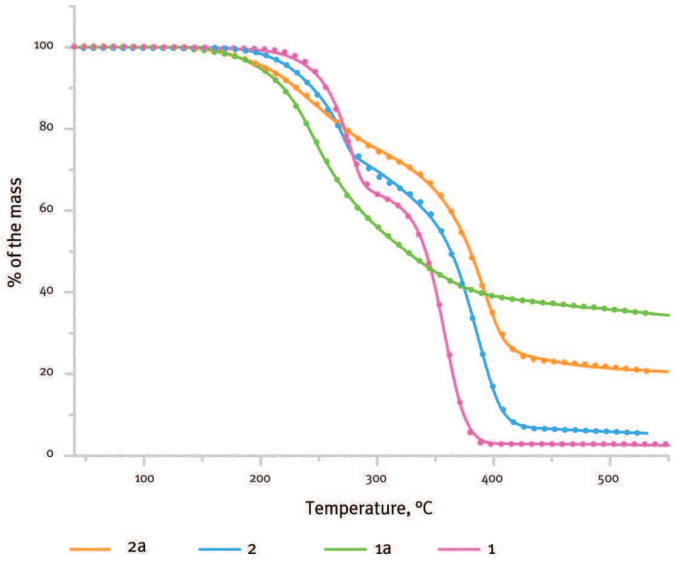

Figure 34. The non-isothermal thermogravimetry runs for aged polyether and polyester urethanes samples 1a-2a, nitrogen, 1-2 are original non-aged samples, the rate of heating 5°C.min^{-1}. The points denote the fit of the experimental run by eq. 14 for j=3. The corresponding rate constants are in Figure 37

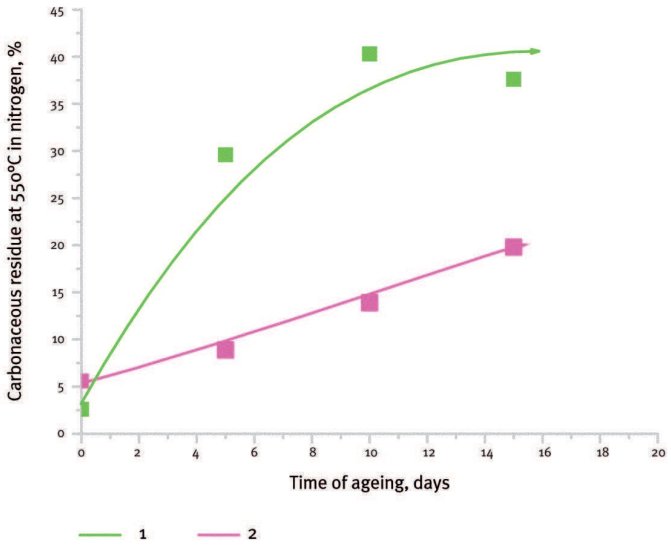

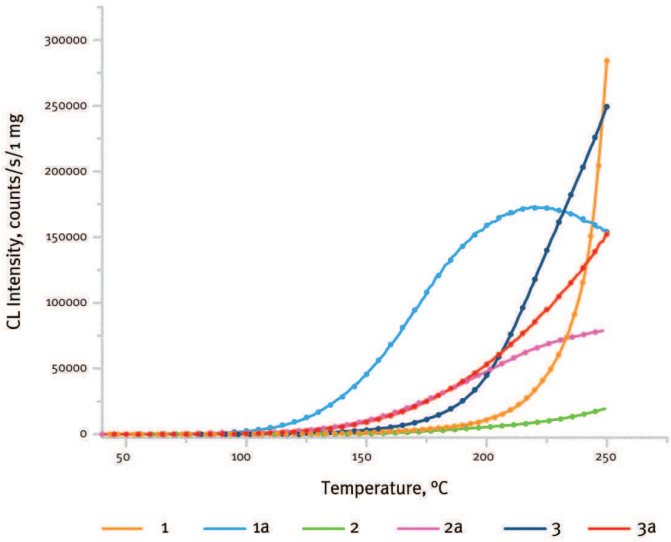

Figure 35. The amount of carbonaceous residue remaining at the pan of TG instrument after sample heating in nitrogen from 40 to 550°C by the rate 5°C.min^{-1}. 1-aged sample of polyurethane 1, 2-aged sample of polyurethane 2

Figure 36. The chemiluminescence intensity runs for aged polyether and polyester urethanes samples 1a-3a (red), oxygen, lines 1-3 are original non-aged samples, the rate of heating 5°C.min^{-1}. Points denote the fit of experimental runs by eq. 11 and 12. The corresponding rate constants are in Figure 37

with reference. One may see that the reference polyether sample 3 gives the faster uptake of the light emission when compared with polyether sample 1. This may be brought about by the oxidation of methylene group in MDI moiety of polyurethane which is converted to carbonyl group with a higher yield of the light emission.

From the set of rate constants on degradation in oxygen (CL) and in nitrogen (TG) which were determined for 100, 200 and 250°C we may see that pre-ageing of polyurethanes leads to the increase of the respective rate constants which is very pronounced in the case of polyether urethane 1 and less significant in the case of polyester urethane 2 and polyether urethane 3. In the latter case the oxidative attack is probably more focused on methylene groups of MDI. The rate constants in nitrogen (TG) are usually lower than those in oxygen (CL) (Figure 37).

While the investigation of the changes of the solid matrix of polyurethanes is the subject of numerous papers, only a few studies are devoted to the formation of volatile organic compounds (VOCs) emitted by polyurethanes (Hakkarainen 2008, Lattuati-Derieux *et al.* 2011; Thiébaut *et al.* 2007; Watanabe *et al.* 2007) during their degradation. Actually, over time, low molecular weight compounds, either degradation products or manufacturing residual products are emitted from the polyurethane matrix and a relationship between the environmental factors (humidity, temperature and daylight), the volatile fraction formed and the bulk polymer composition should be established. From this viewpoint the sample 1 and sample 2 original and artificially aged were examined by using solid phase micro extraction coupled with gas chromatography mass spectrometry

k_{av}	k_{100}, s^{-1}	k_{100}, s^{-1}	k_{200}, s^{-1}	k_{200}, s^{-1}	k_{250}, s^{-1}	k_{250}, s^{-1}
Sample	CL	TG	CL	TG	CL	TG
1	3.9e-7	1e-9	9.8e-5	1.7e-5	3.7e-3	5.1e-4
1a	1.1e-5	3.8e-6	2.1e-3	2.1e-4	1.5e-2	1.3e-3
2	4.8e-6	4.8e-7	5.4e-4	2.3e-6	4.1e-3	5.6e-4
2a	7.6e-6	4.7e-6	1.1e-3	1.4e-4	7.7e-3	4.5e-4
3	1.2e-6		3.8e-4		9.1e-3	
3a	3.7e-6		6.1e-4		4.7e-3	

Figure 37. Average rate constants k_{av} determined from nonisothermal chemiluminescence (CL) and thermogravimetry (TG – eq. 14) measurements of original and light aged (a) samples of polyurethanes 1,2 and 3. Temperatures 100, 200 and 250°C

(SPME-GCMS) and pyrolysis gas chromatography mass spectrometry (Py-GCMS).

In addition to sample 1 and 2, four naturally aged polyurethane foams collected from various daily life objects were examined as well. Sample S1 was taken from a suitcase and visually seemed to be in poor state of conservation. Sample S2 was part of a conditioning box and appears to be in a good state of conservation. Sample S3 was taken from a much degraded chair stuffing. Sample S4 was collected from the back of a chair not exposed to light and also seemed to be in a very good state of conservation. Samples S1 and S3 were yellow and showed a total loss of integrity and a pronounced degradation resulting in powdering.

Morphological changes were followed based on visual examinations (binocular); naturally aged foams were preliminary characterised using attenuated total reflection Fourier transform infrared spectroscopy (ATR-FTIR). Infrared data were also collected from newly made foams after artificial ageing.

Similarly as from chemiluminescence, DSC and thermogravimetry data from all artificially and naturally aged samples, visual observations and Py-GCMS data and in agreement with the literature (Kerr and Batcheller 1993; Szycher 1999) it was confirmed that PUR esters are more sensitive to thermal ageing in humid conditions and hydrolysis and less sensitive to light ageing, while PUR ether degrade primarily by photo-oxidation and have higher resistance to hydrolysis.

The main morphological aspects observed visually and the main degradation compounds analytically characterised from the artificially and naturally aged PUR esters and PUR ethers are summarized in Figure 38. It is interesting to note that artificial and natural ageing were providing similar analytical results and thus, it seems well relevant to use such accelerated ageing to simulate natural degradation processes.

The results are illustrated by the commercial polyurethane ester (Sample 2) and polyurethane ester samples S1 and S2. After eight weeks of ageing in humid condition, the commercial polyurethane

Samples and ageing	Main morphological aspects	Main degradation compounds
ARTIFICIALLY AGED		
Humid ageing of commercial PUR ester (sample 2)		
4-weeks ageing time	Slight weakening and darkening	DEG, TDA, TAI
8-weeks ageing time	Important weakening and darkening. Presence of adipic acid crystals	DEG, TDA, TAI, AA
Light ageing of commercial PUR ether		
120-hours ageing time	Slight yellowing and cracking on the surface	G
240-hours ageing time	Important yellowing, cracking and crumbling resulting in powdering	G
NATURALLY AGED		
S1: PUR ester from suitcase	Poor state of conservation: very yellowed, total loss of coherence resulting in powdering and presence of adipic acid crystals	DEG, TDA, AA
S2: PUR ester from conditioning box	Good state of conservation	DEG, TAI
S3: PUR ether from chair stuffing	Poor state of conservation: very yellowed and total loss of coherence resulting in powdering	G
S4: PUR ether from the back of a chair	Good state of conservation	G

Figure 38. Main morphological aspects visually observed and main degradation compounds analytically characterised by Py-GCMS and SPME-GCMS from the selected artificially and naturally aged foam samples

ester, besides the important loss of mechanical properties and darkening, gives white crystals of adipic acid (AA) which appear inside the pores and on the surface of the foam. Adipic acid crystals were also observed in naturally aged foam S1. Such crystals have been also detected and identified from one polyurethane museum artefact (van Oosten 2002). The Py-GCMS analysis permits to identify potential chemical markers of the polyurethane ester degradation. Figure 39 shows the pyrograms of commercial Sample 2 unaged and artificially aged in humid conditions during 4 and 8 weeks. In the unaged Sample 2, we identified the compounds such as carbon dioxide, adipic ketone (K), diethylene glycol (DEG), 2,4- and 2,6-toluene diisocyanate isomers (TDI) and some adipate derivatives (A) of which chemical structures have not been identified. The adipic ketone (C_5H_8O, MW 84) can originate from the adipic acid raw material (Font 2001, Ohtani 1987). The DEG ($C_4H_{10}O_3$, MW 106), a low molecular weight polyol is used in the polyurethane synthesis either as chain extenders or component of the polyester polyol synthesis. During the artificial ageing, the chromatographic fingerprints become simple and the isocyanate moiety was modified. After four weeks of ageing, in addition to the relative increase of diethylene glycol, the occurrence of toluene amino isocyanate isomers (TAI) and 2,4- and 2,6-toluene diamine isomers (TDA) may be noted. TAI may undergo hydrolysis to TDI (Berlin 2005) and 2,4- and 2,6- toluene diamines are being formed. An increasing release of 2,4- and 2,6-TDA with duration of 2,4- and 2,6-TDI hydrolysis have been reported

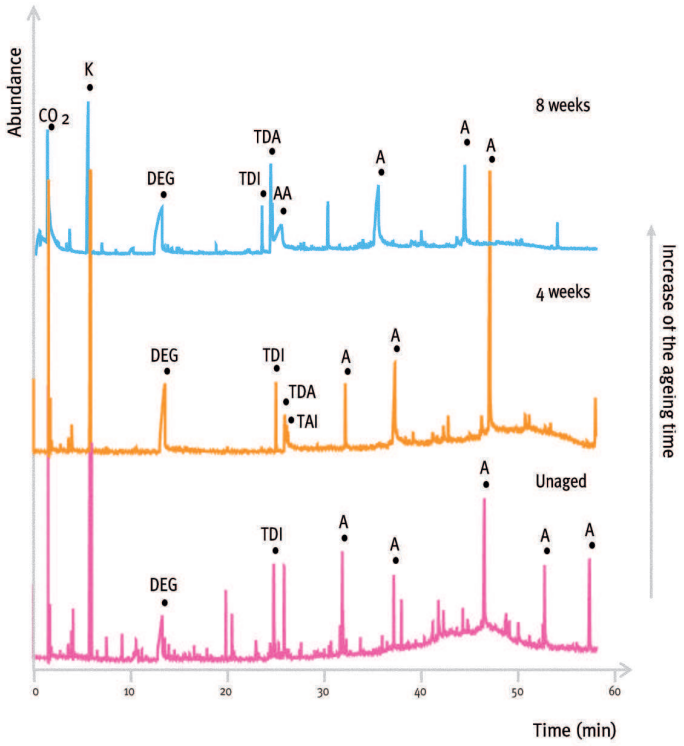

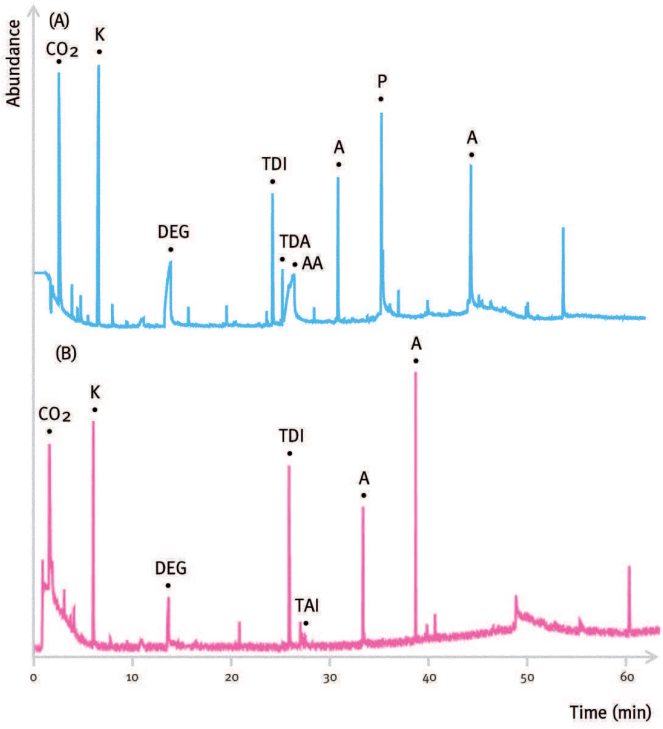

Figure 39 (left). Pyrograms of commercial unaged and artificially aged (in humid conditions) polyester-based polyurethane foams (Sample 2). Compounds marked (•) correspond to: (K) adipic ketone, (DEG) diethylene glycol, (TDI) toluene diisocyanate isomers, (TDA) toluene diamine isomers, (TAI) toluene amino isocyanate isomers, (AA) adipic acid, (A) adipate derivatives, the chemical structures of which have not been identified

Figure 40 (right). Pyrograms of naturally aged polyester-based polyurethane foams collected (A) from a suitcase S1 and (B) from a conditioning box S2. Compounds marked (•) correspond to: (K) adipic ketone, (DEG) diethylene glycol, (TDI) toluene diisocyanate isomers, (TDA) toluene diamine isomers, (TAI) toluene amino isocyanate isomers, (AA) adipic acid, (A) adipate derivatives, the chemical structures of which have not been identified, (P) phthalate esters

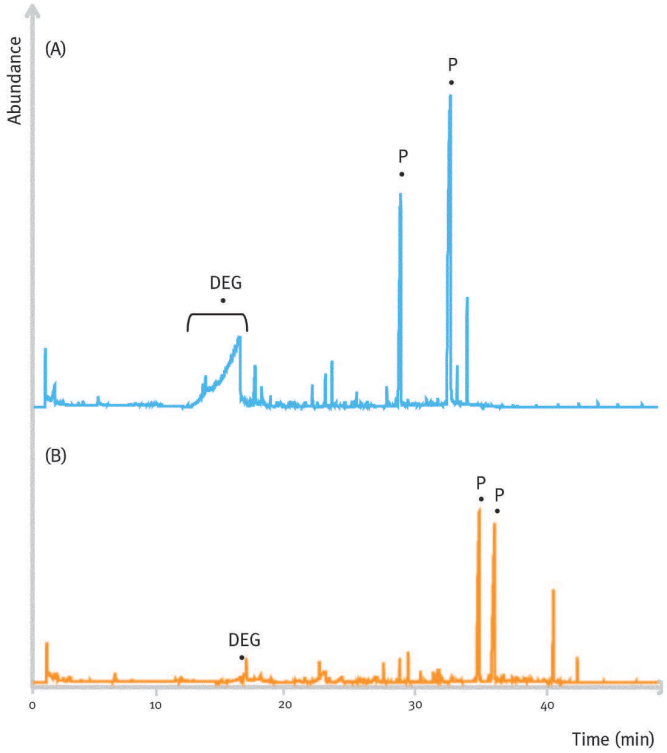

Figure 41. Chromatograms of the SPME extracts from naturally aged polyester-based polyurethane foams collected (A) from a suitcase S1 and (B) from a conditioning box S2. Compounds marked (•) correspond to: (DEG) diethylene glycol, (P) phthalate esters

previously (Lind 1996). After eight weeks of ageing, adipic acid was identified.

Figure 40 presents two Py-GCMS fingerprints of S1 and S2 foams which were in different states of degradation. Pyrograms previously obtained from commercial samples helped us in their identification; they are from poly(diethylene glycol adipate) polyurethanes. Phthalate derivatives (i.e. phthalic acid diisobutyl ester) could originate from plasticisers introduced during the manufacturing process. Sample S1 gave a relatively high amount of diethylene glycol (DEG), 2,4- and 2,6-toluene diamines (TDA) and of adipic acid (AA). Pyrogram of the foam S2 which was in a relatively good state showed a lower amount of diethylene glycol (DEG), presence of toluene amino isocyanate isomers (TAI) and no adipic acid. These results were coherent with those obtained from artificial ageing and therefore the presence of these compounds can be used as degradation markers.

Chromatograms of the SPME extracts from the commercial ester foam artificially aged in humid conditions did not indicate the obvious changes within the VOCs composition except for the presence of diethylene glycol (DEG). Chromatograms of the SPME extracts from naturally aged PUR ester foams were very similar but, the presence of diethylene glycol in different relative amount was noted. Figure 41 presents two SPME fingerprints from foams S1 and S2. The relative increase of diethylene glycol could be correlated with the physical state of the foams.

3.4.2. The progress of degradation in normalized coordinates

As the maximum intensity of chemiluminescence changes from the polymer to the polymer an idea was proposed to plot the respective runs in the normalised coordinate of the intensity. Normalised intensity is the actual intensity divided by the maximum intensity. In such a way intensity at the maximum is equal to 1 and the differences in the lower temperature regions due to sample ageing may well be differentiated.

From the viewpoint of long term stability of polymers, the region of lower temperatures is of higher interest. Uniform approach may be introduced, namely to compare the temperature of the section of normalised graphs up to 10% of the maximum chemiluminescence intensity measured at the beginning and at the end of the polymer exposition. The example may be seen on artificial doll monitoring before and that after 17 months of its exposition in laboratory

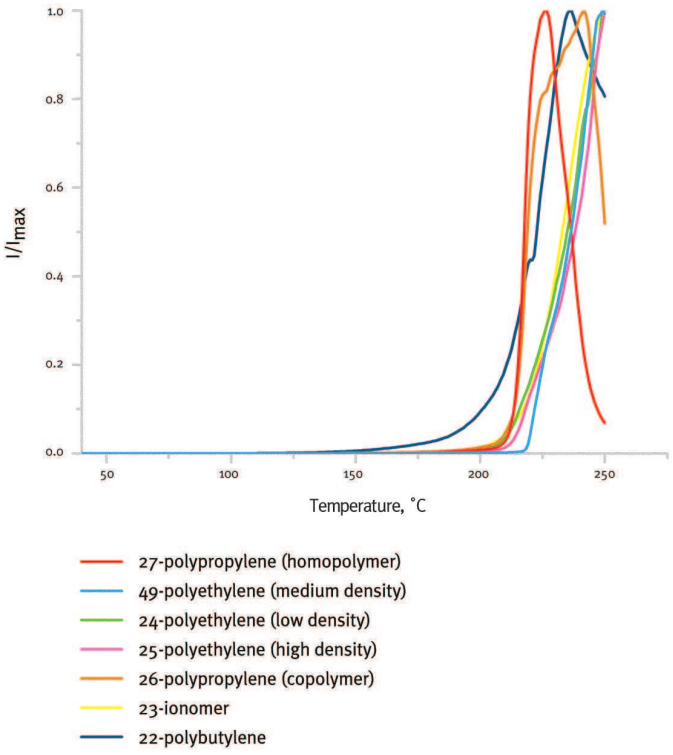

Figure 42. Chemiluminescence from some polyolefins in the ResinKit™ in normalized coordinates

conditions. The most significant changes were observed for polyester urethane foam (shoe of the doll) -32°C, polystyrene head -31°C, polyether urethane foam (shoe of the doll) -23°C and PET body -22°C. The changes on polyurethane foams were already visible (yellowing). The items least touched by ageing were polyamide skirt, acrylic hairs and low density polyethylene arms. The more detailed observations related to the long term ageing of the doll at different locations are reported in the Chapter 2.

3.4.3. CL of polymers in the ResinKit™

Atlas of non-isothermal thermogravimetry, DSC and chemiluminescence was prepared for those wanting to have the fast orientation in the degradation of the respective polymer. Here we present the data on chemiluminescence from the polymers of the ResinKit™ extracted from this Atlas.

All chemiluminescence experiments were carried out in oxygen atmosphere and at the rate of heating 5°C.min^{-1}. The measurements were performed with powders obtained by grinding of corresponding ResinKit™ sample. The example of the chemiluminescence measurements on ResinKit™ hydrocarbon polymers in normalised coordinates is seen in Figure 42 and parameters determined for each item of the ResinKit™ are in the Figure 43.

3.4.4. TGA of ResinKit™ polymers after two years of storage

Polymers in ResinKit™ are usually considered to be rather stable over years when kept under laboratory conditions. This assumption, however, should be taken with some reservation. As it is shown in Figure 44 where non-isothermal DSC and thermogravimetry records are presented for polyolefins from the ResinKit™, thermogravimetry in nitrogen shows the observable shift of corresponding line to lower temperature region after two years of ResinKit™ storage under laboratory conditions. This shift appears the most significant for polypropylene homopolymer which belongs to polymers which are rather sensitive to the oxygen effect. Thermogravimetry line observed in oxygen may be found at temperatures more than 100°C below that in nitrogen.

Jozef Rychlý, Lyda Rychlá and Agnès Lattuati-Derieux

ResinKit™ No.	Polymer	Temperature of the 10% uptake of CL intensity – compared to the maximum, °C	Maximum CL intensity I_{max}, counts/s/1 mg
1	Polystyrene (general purpose)	221.7	24 861
2	Polystyrene (medium impact)	181.6	34 642
3	Polystyrene (High impact)	180.0	50 597
4	Styrene Acrylonitrile (SAN)	194.2	145 313
5	Acrylonitrile-butadiene-styrene (ABS) – transparent	181.7	224 036
6	Acrylonitrile-butadiene-styrene (ABS) – medium impact	192.5	707 706
7	Acrylonitrile-butadiene-styrene (ABS) – high impact	196.7	443 846
8	Styrene butadiene block copolymer	223.4	73 228
9	Acrylic	167.5	5 905
10	Modified acrylic	195.0	157 412
11	Cellulose acetate	209.9	423 922
12	Cellulose acetate butyrate	208.3	499 309
13	Cellulose acetate propionate	189.0	490 210
14	Nylon (transparent)	194.9	703 760
15	Nylon type 66	175.0	2.1e6
16	Nylon type 6	165.0	2.08e6
17	Thermoplastic polyester (PBT)	225.8	79 407
18	Thermoplastic polyester (PETG)	194.2	122 804
19	Polyphenylene oxide (PPO)	201.7	134 552
20	Polycarbonate	158.3	20 067
21	Polysyulfone	160.8	15 389
22	Polybutylene	221.8	109 036
23	Ionomer	217.5	211 091
24	Polyethylene (low density)	215.7	1.24e6
25	Polyethylene (High density)	218.3	1.0e6
26	Polypropylene (Copolymer)	213.7	1.09e6
27	Polypropylene (Homopolymer)	213.8	1.83e6
28	Polypropylene (Baryum sulfate reinforced)	198.0	1.4e6
29	Poly(vinyl chloride) (PVC flexible)	182.3	29 628
30	Poly(vinyl chloride) (PVC rigid)	188.3	18 825
31	Acetal resin (homopolymer)	209.2	903 323
32	Acetal resin (copolymer)	203.2	85 017
33	Polyphenylene sulfide (PPS)	146.6	84 062
34	Etylene vinyl acetate copolymer (EVA)	228.7	399 982
35	Synthetic elastomer (Styrene block copolymer)	179.2	93 228
36	Polypropylene (glass filled)	212.5	1.04e6
37	Urethane elastomer, thermoplastic (TPU)	205.0	13461
38	Polypropylene (Flame retardant)	246.1	651 158
39	Polyester elastomer	220.0	886 800
40	Acrylonitrile butadiene styrene (ABS) flame retardant	185.8	125 133
41	Polyallomer	221.7	1.29e6
42	Styrene terpolymer	196.7	269 442
43	Polymethyl pentene	237.5	1.03e6
44	Polypropylene (Talc reinforced)	208.1	457 142
45	Polypropylene (Calcium carbonate reinforced)	192.8	551 219
46	Polypropylene (Mica reinforced)	197.2	371 297
47	Nylon type 66 – 33% glass	155.8	703 760
48	Thermoplastic rubber (TPV)	214.2	238 687
49	Polyethylene (medium density)	222.3	1.6e6
50	Acrylonitrile butadiene styrene (ABS) nylon alloy	190.4	907 328

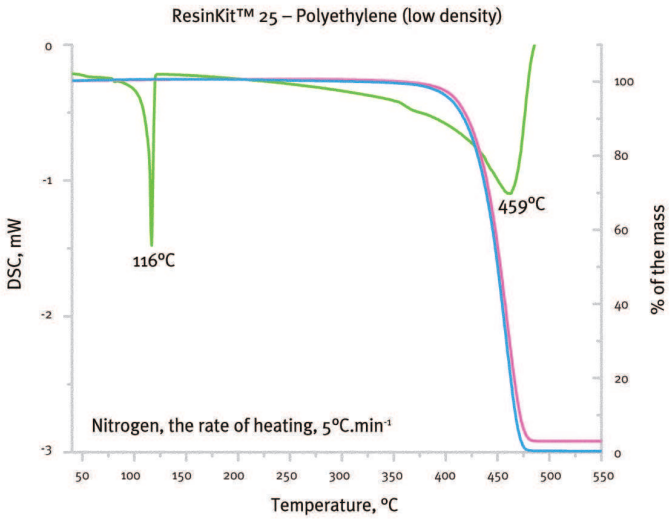

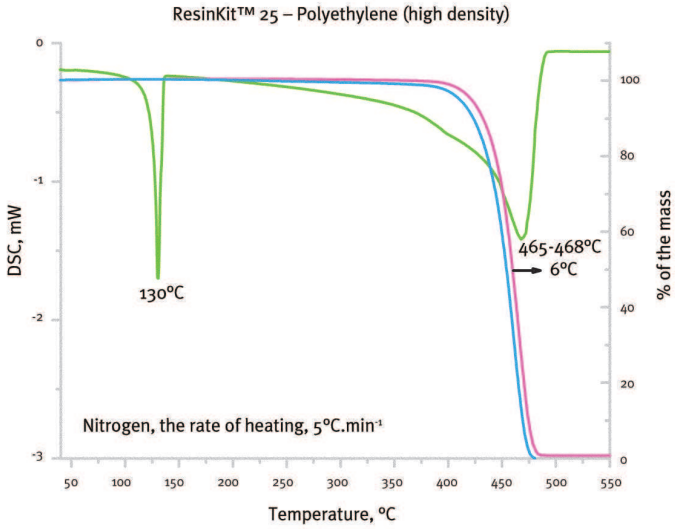

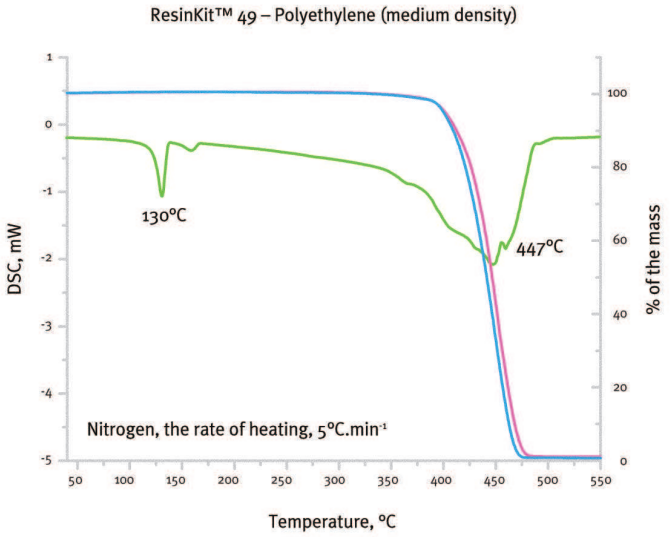

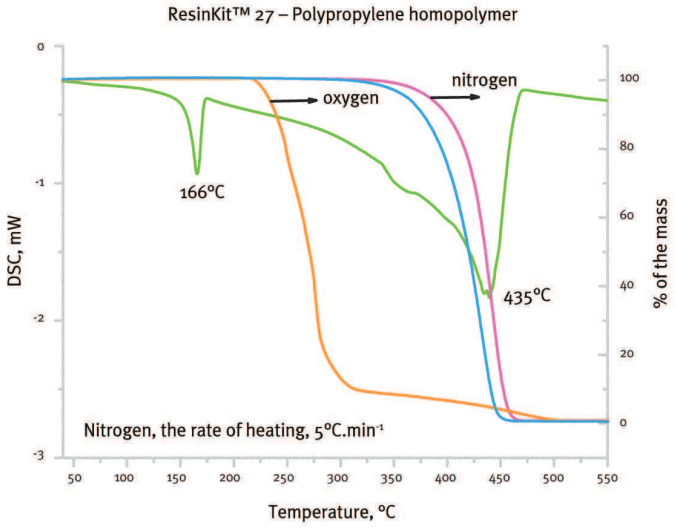

Figure 43 (preceding page). Parameters from non-isothermal chemiluminescence of polymers from ResinKit™

Figure 44. Nonisothermal thermogravimetry in nitrogen (magenta line) of some ResinKit™ polymers after two years (blue lines) of the storage in air at laboratory conditions. Green line represents the corresponding DSC record. The orange line shows the comparison with degradation in oxygen